Electromagnetics

Torque Performance Calculation of a Novel Magnetic Planetary Gear

Rong-Jie Wang[1*], Alexander Matthee[1], Stiaan Gerber[1**], Pushman Tlali[1**]

[1] *Department of Electrical and Electronic Engineering, Stellenbosch University, Stellenbosch, South Africa*
[*] *Senior Member, IEEE*
[**] *Member, IEEE*

Abstract– In this paper, an efficient energy-based methodology is proposed for calculating the torque performance of a novel magnetic planetary gear. To verify the proposed method and the gear performance, a prototype was also constructed and experimentally evaluated. It shows good agreement between the predicted and measured torque performance. The new gear topology demonstrates higher torque capability than the common, flux-modulated magnetic gear. However, the complex mechanical construction and the high loss at no-load remain as challenges.

Index Terms– Electromagnetics, magnetic gears, magnetic stored energy, torque calculation

I. INTRODUCTION

Magnetic gears (MGs) are receiving increasing attention from both research institutions and industry. Different high performance magnet gear technologies, such as flux modulated [Atallah 2001], harmonic [Rens 2007] and planetary [Huang 2008] magnetic gears, have been proposed in the past 15 years. Recently, a new magnetic planetary gear has been proposed in [Davey 2016], which shows the potential of even higher torque capability than that of a flux modulated magnetic gear (FMMG). In this study, an efficient energy-based calculation method is proposed for predicting the performance of the new gear. A working prototype was developed and experimentally investigated to validate the operating performance of the new gear and the proposed method.

II. MAGNETIC PLANETARY GEARS

The layout of a mechanical planetary gear consisting of a sun gear, a ring gear and a carrier with planet gears is shown in Fig. 1(a). Typically, one of these three components is kept stationary while the other two components act as input and output, respectively. The resultant gear ratio depends on the pitch radii of the components, which are proportional to their respective number of teeth, and on which component is stationary. The relationship between the number of teeth of the ring gear (z_r), sun gear (z_s) and planet gear (z_p) is governed by:

$$z_r = z_s + 2z_p \tag{1}$$

The general angular velocity relationship between the sun gear (ω_s), ring gear (ω_r) and planet carrier (ω_c) is:

$$\omega_s z_s + \omega_r z_r = \omega_c (z_s + z_r) \tag{2}$$

The operating principle of MGs is very similar to mechanical gears except that all the gear teeth are replaced with permanent magnets (PMs) [Gouda 2011]. For a common magnetic planetary gear, the pole-pairs of the sun, ring and planet gears generally satisfy the same relationship as in eqn. (1). The pole pitch of each MG component should be the same and the number of planet gears should be carefully selected to maintain synchronization [Huang 2008]. For example, a magnetic planetary gear with $z_r = 12$, $z_s = 6$ and $z_p = 3$ is shown in Fig. 1(b).

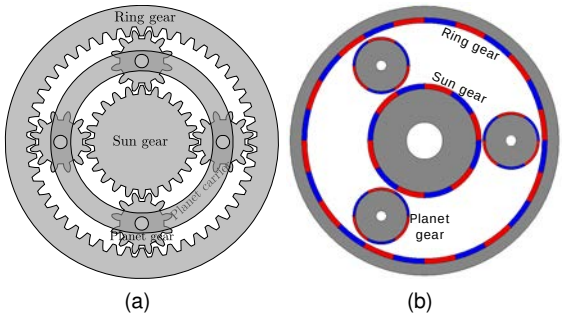

Fig. 1. Layout of (a) a mechanical, and (b) a magnetic planetary gear.

Consider one arrangement where the planet carrier is stationary and the sun gear is the input gear. The planet gears simply rotate about their own axes at a rate determined by the ratio of the number of teeth (z_s/z_p). The rotation of the planet gears can, in turn, drive the ring gear in a corresponding ratio (z_p/z_r). Thus, with a stationary planet carrier ($\omega_c = 0$), the resultant gear ratio (G_e) of the planetary gear is simply ($-z_s/z_r$) [Niguchi 2012], where the negative sign indicates that the sun and ring gears rotate in opposite direction.

For mechanical and common magnetic planetary gears with stationary carriers, G_e is still related to z_p, because of eqn. (1). By making use of flux modulation effects, unconventional magnetic planetary gear designs can be realized, where the planet gears can be replaced by either ($z_r + z_s$) ferromagnetic pole pieces [Atallah 2001] or the same number of free-rotating flux-switching planet magnets [Davey 2016]. The same angular velocity relations as in eqn. (2) can be obtained [Gouda 2011]. Figure 2 illustrates the layout of the new magnetic planetary gear topology, where the ring and sun gears contain 21 pole pairs and 2 pole pairs, respectively, and the planet carrier has 23 freely-rotating 2-pole hollow planet gear magnets to enhance the flux modulating effects [Davey 2016].

III. TORQUE PERFORMANCE CALCULATION

Since each planet gear deals with the torques from both sun and ring gears, a unique stable position exist for each planet gear, which corresponds to the minimum stored energy as shown in Fig. 2. Obviously, the calculation of the torque

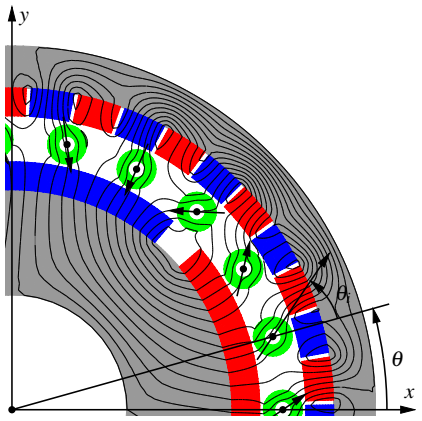

Fig. 2. The new magnetic gear topology showing the magnetization vector angle θ_i of a planet gear relative to its position angle θ.

characteristics of the magnetic planetary gear would require the knowledge of the angular positions of these planet gears. Although two torque calculation methods are proposed in [Davey 2016], they both have relatively slow convergence performance. In this paper, an energy-based finite element (FE) calculation method is proposed, which assumes that:

- The total magnetic stored energy in the gear should be minimum (*or maximum magnetic co-energy*) when all the planet gears settle in their equilibrium positions
- There exists a unique balanced angular position for each planet gear to meet with the previous condition, where the net torque on a planet gear is zero

A. FE Modeling Techniques

Since there is no magnetic periodicity that can be exploited in the FE simulation of this gear design, the full gear needs to be modeled. If the rotational movement of each planet gear is incorporated into the FE modeling, it would drastically increase the computational efforts and the complexity of the FE model. A simpler approach would be to parametrize the magnetization vector, $\mathrm{M}(\vec{\theta}_i)$, for each planet gear and rotate these vectors instead, while keeping the mesh constant. In this case, there are 23 localized magnetization vectors (one for each planet gear), which are used as variables. The angles of these vectors (θ_i) can be found by solving an unconstrained optimization problem as follows:

$$\mathcal{F} = \mathrm{MIN}\{\mathrm{W_{en}}[\mathrm{M}(\vec{\theta}_i)]\},\ i = 1,\ 2,\ \ldots,\ 23 \tag{3}$$

where the magnetic stored energy, $\mathrm{W_{en}}$, is computed by integrating the energy density of the whole 2D FE model:

$$\mathrm{W_{en}} = \iint \mathbf{H} \cdot \mathbf{dB}\, dS \tag{4}$$

A flowchart of the computation process is shown in Fig. 3, in which VisualDOC, a multidisciplinary optimization software from VR&D, is used as the optimization environment and it couples with a 2D FE program to find the angles of magnetization vectors. To improve the computational efficiency and reduce the risk of converging to a local optimum, several preconditioning techniques were implemented, i.e.:

(i) presetting the magnetization vectors $\mathrm{M}(\vec{\theta}_i)$ radially according to the sun gear's flux pattern,

(ii) presetting $\mathrm{M}(\vec{\theta}_i)$ using the angles obtained from the flux-tracing FE run with non-magnetized planet gears, and

(iii) presetting $\mathrm{M}(\vec{\theta}_i)$ according to $\theta_i = z_s\theta$, where θ is the angular position of a planet gear. This interesting linear relation appears when the optimization is formulated for $\mathrm{MAX}\{\mathrm{T_{gear}}(\vec{\theta}_i)\}$ instead of eqn. (3).

The purpose is to establish the near-optimum θ_i for the subsequent optimization routine. Since it is an unconstrained optimization problem, a gradient-based Broydon-Fletcher-Goldfarb-Shanno (BFGS) algorithm was used. Figure 4(a) compares the performance of the implemented time-reduction techniques, which shows that the proposed techniques are more efficient than the one without preconditioning, and a clear sign of convergence is evident after merely 2 iterations. Figure 4(b) displays the computed θ_i of each planet gear at the stall torque position. The worst net torque on a planet gear for these θ_i is found to be 0.067 Nm. Figure 5 shows the spatial harmonic distributions of the inner and outer air-gap fluxes when all the PMs are active and when only the planet PMs are active, respectively. The flux modulation effects of the planet PMs on the working harmonics (2^{nd} order and 21^{st} order) is evident.

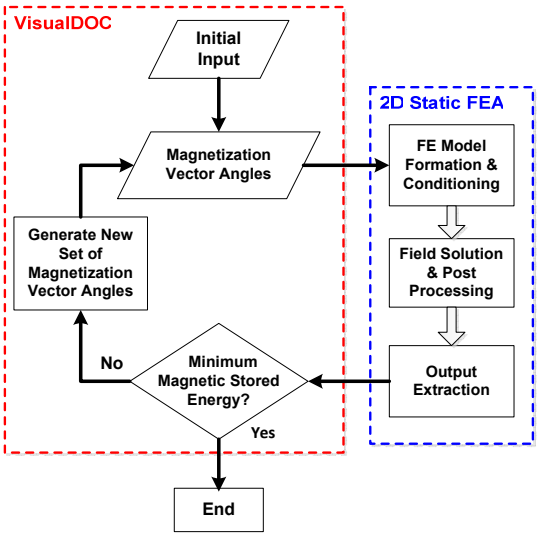

Fig. 3. Flow chart of the computation process.

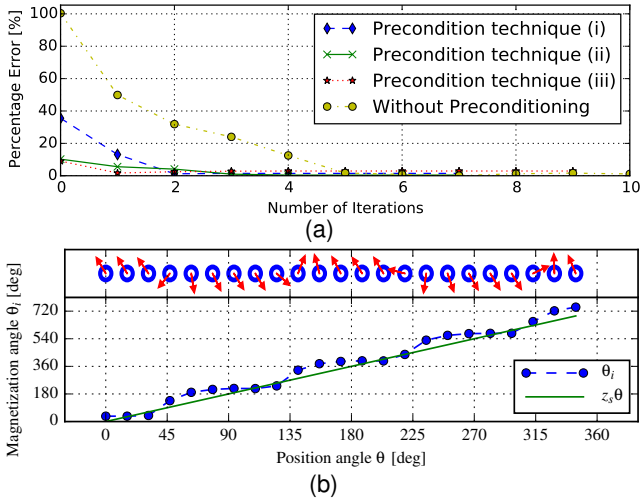

Fig. 4. (a) Convergence comparison between different time reduction techniques; (b) Computed magnetization vector angle (θ_i) relative to its respective position angle (θ) at the stall torque position.

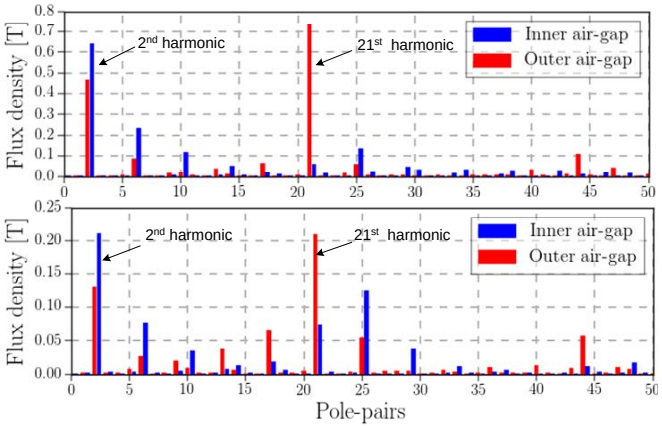

Fig. 5. Spatial harmonic distributions of the inner and outer air-gap fluxes when all the PMs are active (top) and when only the planet PMs are active (bottom).

B. Torque Calculation

With the angles of the magnetization vectors known, the torque at a specific gear position can be readily calculated. To facilitate the FE modeling of the gear movement, the moving band solver described in [Davat 1985, Antunes 2004, Gerber 2015] was also implemented. Since Coulomb's virtual work method is known for its high accuracy and requires only one solution [Coulomb 1983, Sadowski 1992], it was implemented for the torque calculation as follows:

$$T = \frac{L}{\mu_0} \sum_{e=1}^{N_{mb}} \int_{\Omega_e} \left(-\mathbf{B}^{\mathbf{T}} \mathbf{G}^{-1} \frac{\partial \mathbf{G}}{\partial \theta} + \frac{\mathbf{1}}{\mathbf{2}} \frac{B^2}{|\mathbf{G}|} \frac{\partial |\mathbf{G}|}{\partial \theta} \right) d\Omega \quad (5)$$

where $\mathbf{B} = [B_x, B_y]$, $B = |\mathbf{B}|$, $\mathbf{G}$ is the Jacobian matrix of the global nodal coordinates relative to the local element coordinates, $|\mathbf{G}|$ is the determinant of $\mathbf{G}$, Ω_e is the area of an element, and N_{mb} is the number of elements in a moving band. To find the torque-angle characteristics of the MG, the sun gear is kept fixed while the ring gear is rotated by a small angle, and a new set of magnetization vectors of the planet magnets were obtained by solving the optimization problem in eqn. (3). The ring gear was rotated again by the same amount and the magnetization vectors were updated for the torque calculation. This process was repeated until the accumulated angle of rotation was twice the pole-pitch angle of the ring gear. A full cycle of the torque versus ring gear position can thus be generated.

IV. PROTOTYPE DEVELOPMENT

For performance benchmarking and cost savings, the PM rotors of a previously developed FMMG [Matthee 2015] were used as ring and sun gears for the magnetic planetary gear. Thus, both gears have exactly the same dimensions despite the difference in the flux modulator/planet carrier. The detailed design parameters are given in Table 1.

Due to the manufacturing difficulties, each 40 mm long cylindrical hollow PM was assembled from two 20 mm cylindrical magnets which were magnetically aligned using an external magnetic field and bonded in position with a strong adhesive. To allow for free rotation as well as better structure strength each planet magnet is supported by a stainless steel shaft as shown in Fig. 6(a). These planet gears are then inserted into slots of a carrier shown in Fig. 6(b). The planet carrier is made of an acetal copolymer material since it needs to be non-magnetic, free from core losses and of good strength and stiffness. In addition, a stainless steel ring was added to strengthen the carrier as shown in Fig. 7(a). The gear and main components are shown in Fig. 7(a)-(d).

Table 1. Design parameters of the magnetic planetary gear

Parameter	Value
Sun gear PM pitch [fraction of pole pitch]	0.9
Sun gear yoke thickness [mm]	18.8
Sun gear PM thickness [mm]	5
Sun gear air-gap length [mm]	0.7
Planet gear PM outer diameter [mm]	7
Planet gear inner diameter [mm]	3
Ring gear PM pitch [fraction of pole pitch]	0.897
Ring gear air-gap length [mm]	0.5
Ring gear PM thickness [mm]	5
Ring gear yoke outer diameter [mm]	130
Number of sun gear pole pairs	2
Number of ring gear pole pairs	21
Number of planet gears	23
Gear ratio	10.5
Stack length [mm]	40
Material for the yoke of sun gear	Mild steel (solid)
Magnet material and grade	NdFeB (N35H)
Material for the yoke of ring gear	M19 (laminated steel)

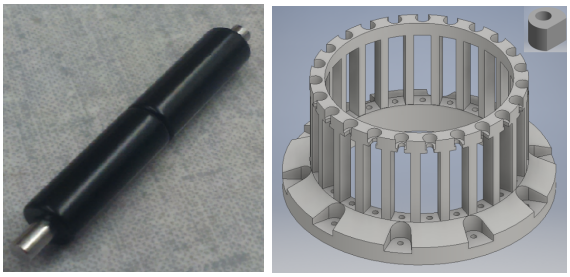

(a) (b)

Fig. 6. Planet gear assembly design (a) an assembled planet magnet on a stainless steel shaft, and (b) planet carrier.

V. PERFORMANCE EVALUATION

A. Torque-angle Characteristics

The torque-angle characteristics of the magnetic planetary gear was measured with the sun gear stationary. A torque was applied to the ring gear in a stepwise fashion via a torque sensor. The measured and simulated torque angle characteristics are compared in Fig. 8, and show good agreement. The measured stall torque of the gear is 74 Nm, which is about 60% more than that of the previous FMMG [Matthee 2015]. Table 2 compares the torque performance between this new magnetic planetary gear and the previous FMMG.

B. No-load Losses

The measured no-load loss (including windage, friction, core and magnet losses) of the magnetic planetary gear at different speeds is plotted in Fig. 9. It can be seen that the no-load loss of the gear exceeds 200 W at 1000 rpm, which is significantly higher than the previous FMMG. These high losses

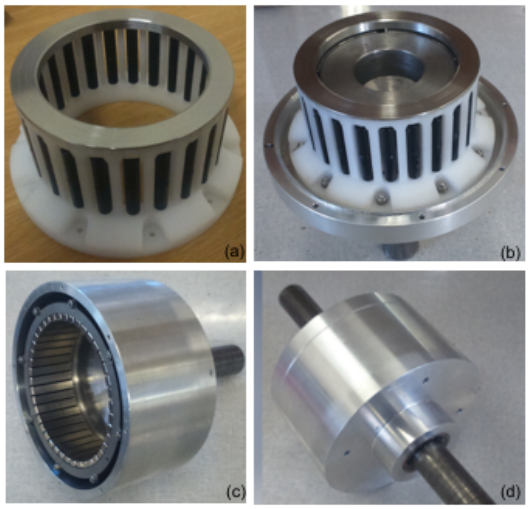

Fig. 7. Main components and assembly of the magnetic planetary gear, showing (a) complete planet carrier with a stainless steel supporting ring; (b) sun gear and planet carrier sub-assembly; (c) ring gear sub-assembly; (d) the assembled complete magnetic planetary gear.

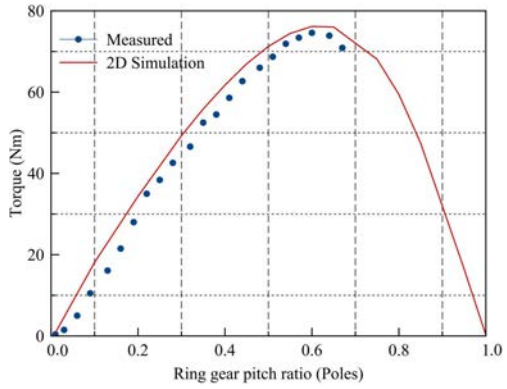

Fig. 8. Measured and simulated ring gear torque-angle characteristics.

are somewhat expected as the rotation mechanism of the planet gears in the carrier is similar to that of bush bearings. Therefore the friction loss between the planet gear shafts and the planet carrier can be quite high. To reduce these losses, high-efficiency bearings could be used, which unfortunately increases the number of maintenance components.

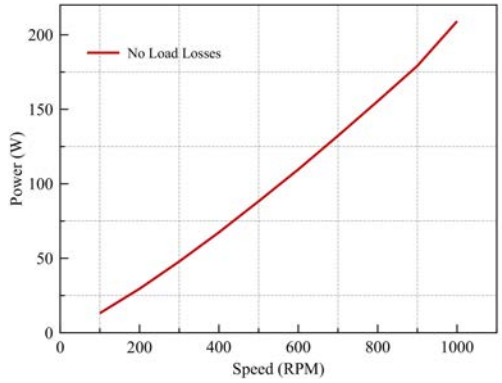

Fig. 9. No-load losses of the novel magnetic planetary gear.

C. Load Tests

Figure 10 shows the test setup for load tests, in which the magnetic planetary gear is connected between a brushless dc motor drive (the prime mover) and a magnetically geared PM generator [Tlali 2016] (the load machine) feeding a 3-phase variable resistance load. The load tests were performed at different speeds ranging from 100 rpm to 1000 rpm (on the sun gear side). At every speed interval the load is adjusted to vary the torque on the ring gear shaft at intervals of 10 Nm starting at 10 Nm to a maximum value of 50 Nm. An efficiency map of the load tests is shown in Fig. 11. Owing to high friction losses, the overall efficiency is not high.

Table 2. Comparison of torque performance

Performance	Planetary MG	FMMG
Stall torque predicted (2D FE)	76 Nm	54.6 Nm
Stall torque (measured)	74 Nm	46.2 Nm
Gear's active volume	531×10^{-6} m^3	531×10^{-6} m^3
Torque density (measured)	139.4 kNm/m^3	87 kNm/m^3
PM material used	1.0225 kg	0.8086 kg
Torque / PM mass (measured)	72.4 Nm/kg	57.1 Nm/kg

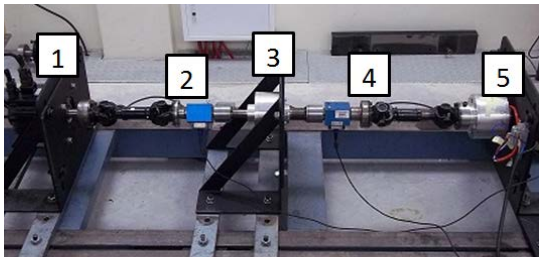

Fig. 10. Load test setup, where 1- motor drive, 2- torque sensor, 3- magnetic gear, 4- torque sensor, 5- an outer-stator magnetically geared PM generator as load machine.

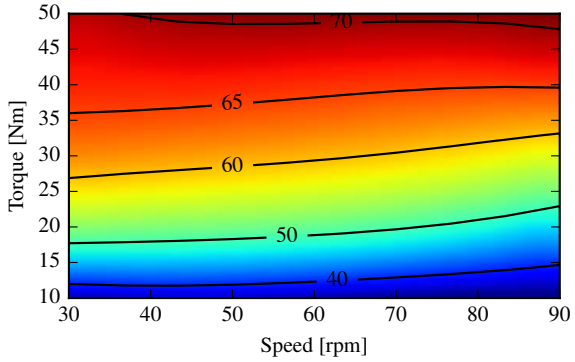

Fig. 11. Efficiency map of the load test results.

VI. CONCLUSION

In this paper, an efficient energy-based performance calculation methodology is proposed for a novel planetary gear. To validate the gear performance and the proposed method, a working prototype has been successfully developed and experimentally evaluated. Close agreement between the predicted and measured results has been achieved. The torque density of the new planetary magnetic gear is nearly 60% higher than that of the same-sized FMMG. Although the new gear topology requires more PM material, the magnet utilization factor (torque/PM mass) is also higher. The challenges of the new gear topology include mechanical complexity, a large number of moving parts, and the associated losses. Further research and development is necessary to establish the true potential of this fascinating design.

ACKNOWLEDGEMENT

This project was supported in part by a National Research Foundation IFRR grant, the Tertiary Education Support Program of ESKOM, and SASOL Technology, all of South Africa. The authors would also like to acknowledge the contribution by Mr J Meeske, Mr P Petzer and Mr A Swart for the construction of the prototype.

REFERENCES

Antunes O, Bastos J, Sadowsk N (2004), "Using high-order finite elements in problems with movement," *IEEE T-MAG, 40(2):529-532*.

Atallah K, Howe D (2001), "A novel high-performance magnetic gear," *IEEE T-MAG, 37(4):2844-2846*.

Coulomb J (1983), "A methodology for the determination of global electromechanical quantities from a finite element analysis and its application to the evaluation of magnetic forces, torques and stiffness," *IEEE T-MAG, 19(6):2514-2519*.

Davat B, Ren Z, Lajoie-Mazenc M (1985), "The movement in field modeling," *IEEE T-MAG, 21(6):2296-2298*.

Davey K, et al. (2016), "Rotating cylinder planetary gear motor," *IEEE T-IA, (early access)*.

Gerber S, Wang RJ (2015), "Evaluation of movement facilitating techniques for finite element analysis of magnetically geared electrical machines," *IEEE T-MAG, 51(2):7400206*.

Gouda E, Mezani S, Baghli L, Rezzoug A (2011), "Comparative study between mechanical and magnetic planetary gears," *IEEE T-MAG, 47(2):439-450*.

Huang C, Tsai M, Dorrell D, Lin B (2008), "Development of a magnetic planetary gearbox," *IEEE T-MAG, 44(3):403-412*.

Matthee A, Gerber S, Wang RJ (2015), "A high performance concentric magnetic gear," *Proc. of Southern African Universities Power Engineering Conference, Johannesburg, South Africa, pp.203-207*.

Niguchi N, Hirata K (2012), "Transmission torque analysis of a novel magnetic planetary gear employing 3-D FEM," *IEEE T-MAG, 48(2):1043-1046*.

Rens J, Atallah K, Calverley SD, Howe D (2007), "A novel magnetic harmonic gear," *IEEE Int. Electric Machines Drives Conf. (IEMDC), 1:pp.698-703*.

Sadowski N, Lefevre Y, Lajoie-Mazenc M, Cros J (1992), "Finite element torque calculation in electrical machines while considering the movement," *IEEE T-MAG, 28(2):1410-1413*.

Tlali P, Gerber S, Wang RJ (2016), "Optimal design of an outer-stator magnetically geared permanent magnet machine," *IEEE T-MAG, 52(2):8100610*.